20th International Sacramento Peak Summer Workshop
Advanced Solar Polarimetry - Theory, Observation, and Instrumentation
ASP Conference Series, Vol. 236, 2001
M. Sigwarth, ed.

An Example of Reconnection and Magnetic Flux Recycling near the Solar Surface[1]

S. R. O. Ploner, M. Schüssler, S. K. Solanki

Max-Planck-Institut für Aeronomie, D-37191 Katlenburg-Lindau, Germany

A. S. Gadun

Main Astronomical Observatory of Ukrainian NAS, Goloseevo, 252650 Kiev-22, Ukraine

Abstract. We discuss an example of 'flux recycling' as seen in MHD simulations of the layers around the solar surface: convective motions bend two initially vertical flux elements of opposite polarity towards each other until they reconnect. The resulting flux loop then rises and the initial situation is restored. During this process, 'new' flux is neither created nor brought into the system from outside. The corresponding synthetic magnetogram, however, suggests the annihilation of two flux elements followed by the later emergence of magnetic flux at another location. Similar recycling events could contribute to the large flux emergence rates observed on small spatial scales.

1. Introduction

Observations with ever increasing spatial and temporal resolution reveal an ever more dynamic sun. In order to improve the understanding of the processes underlying the observed phenomena, comprehensive numerical simulations including as much physics as possible are carried out. The potential power of such simulations is obvious: observations sample the physical quantities indirectly and invariably involve non-linear averaging both over depth and space. In contrast, simulations provide direct access to all involved physical quantities at each mesh point within the computational domain.

2. Numerical Method

The code used for this numerical experiment is an extension to MHD (cf. Brandt & Gadun 1995) of the hydrodynamic code describing a fully compressible, gravitationally stratified, and radiatively coupled plasma (Gadun et al. 1999). The

[1]In memorium of Aleksey S. Gadun who unexpectedly deceased shortly after a visit to Lindau during which this model was calculated.

Figure 1. Eight snapshots (separated by 2 min each) of the full computational domain displaying the magnetic field (solid lines) and the velocity field (arrows). The thick horizontal lines indicate the levels $\log(\tau) = -0.5$ and 0.5, from top to bottom, respectively (τ is the continuum opacity at $\lambda = 5000$ Å). For reference to Fig. 3, the sequence starts at $t = 85$ min.

radiative heating term is determined within the grey approximation (cf. Gadun 1995).

The magnetic field is described by means of the vector potential, thus guaranteeing that the field is divergence-free within the computational domain. In contrast to other studies (e.g. Nordlund & Stein 1989, Steiner et al. 1998) the initial magnetic field is of mixed polarity with a bipolar structure. The initial field is introduced into a fully relaxed solution of a non-magnetic simulation. In order to relax the model from this inconsistent state we run the code for 30 minutes solar time and start to analyze its output thereafter.

The lateral boundaries are periodic whereas the lower and upper boundaries are open so that, e.g., mass can flow in and out. The field and the velocity are kept vertical there. Additionally, the total pressure is held constant at the bottom.

The most important simplification is the reduction to two spatial dimensions which allows us to simulate in larger spatial domains and over longer times than is possible in a 3D simulation. Note that many phenomena of 3D convection are well described in 2D simulations (Steffen & Freytag 1991, Gadun et al. 1999, Ploner et al. 1999) although some observations are less accurately reproduced. The computational domain (CD) covers horizontally 5000 km and allows several granules to coexist. The vertical extent is 1600 km and the resolution is 25 km in both spatial dimensions. The run covers about 3 h solar time with an adaptive temporal resolution of at least 0.025 s. For a comprehensive description of the numerical methods we refer to Ploner et al. (2001).

3. Results

3.1. An example of flux recycling

Figure 1 shows a temporal sequence of 8 snapshots, separated by 2 min each, displaying the full CD. In the first snapshot (Fig. 1a) we have two strong, nearly vertical flux concentrations (flux sheets, FSs) with a field strength around 1500 G at $\tau = 1$. This situation evolved after 85 min solar time (compare with Fig. 3).

The dynamics of the FSs is dominated by the surrounding convective motions. As the pressure within the granule located around $x = 1.0$ Mm decreases, the two adjacent granules start to dominate and the resulting counter-directed horizontal flows both incline the FSs and bring them closer together (Fig. 1b and c). The FSs become kinked at or below the surface region but remain nearly vertical in the atmospheric layers. As soon as the two FSs have been moved sufficiently close to each other, the field lines begin to reconnect rapidly due to their opposite polarity. Within less than 2 min a magnetic arch forms in the

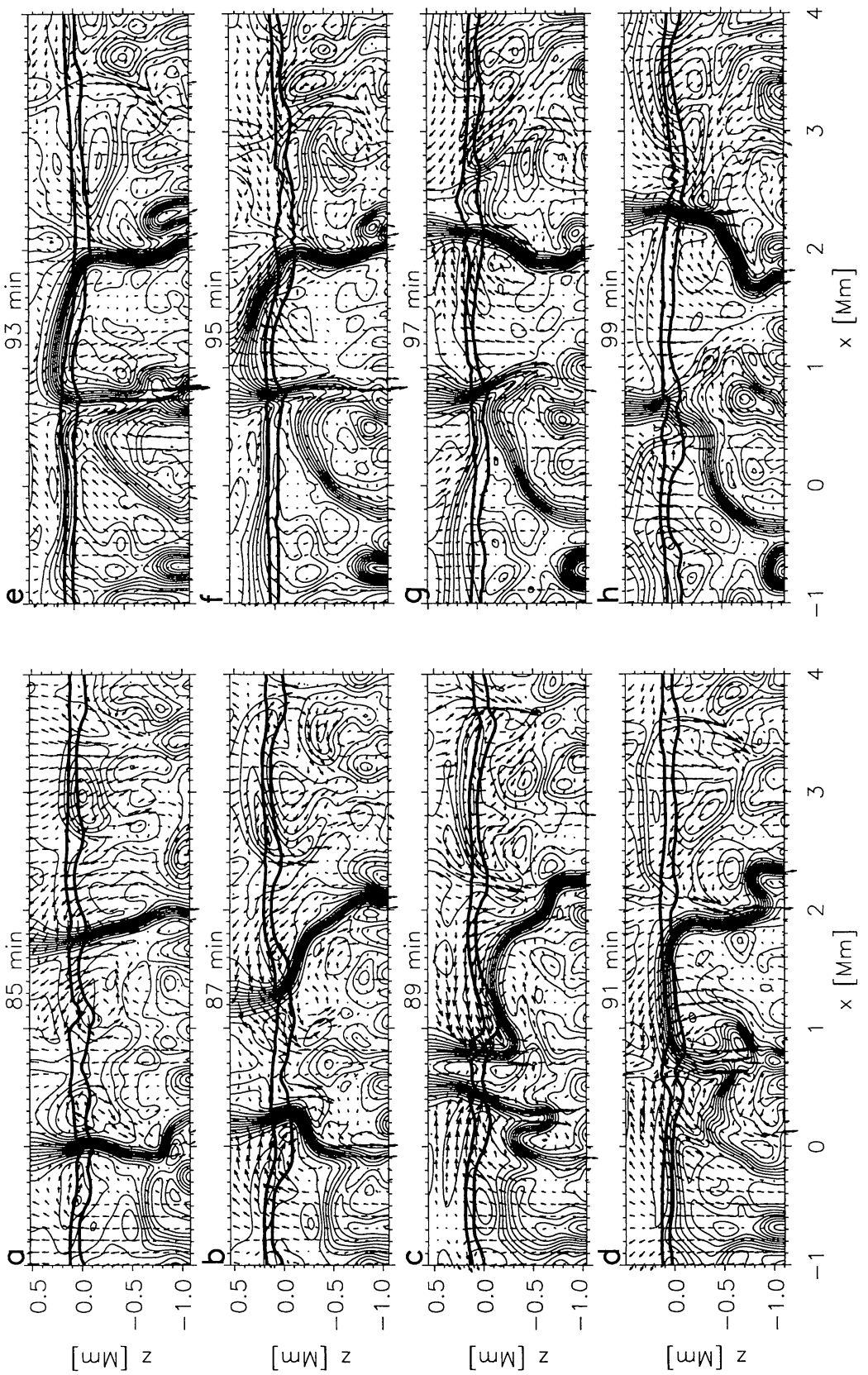

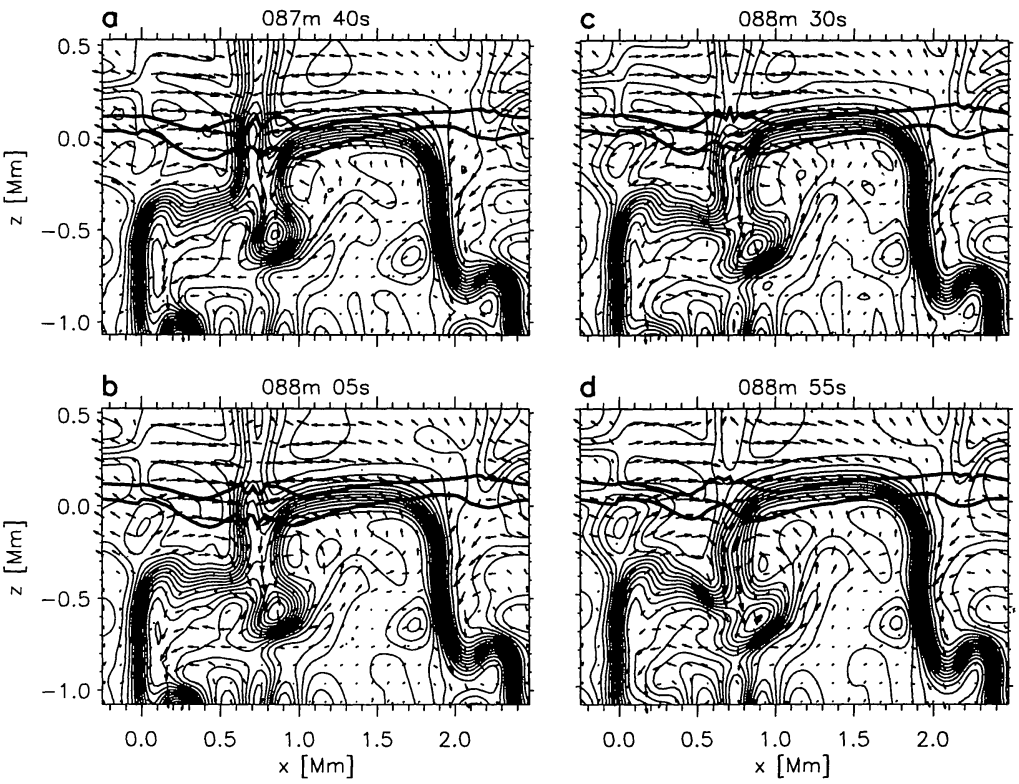

Figure 2. Evolution of part of the reconnection process seen between Fig. 1c and d plotted at higher temporal resolution. The 4 frames are separated by 25 s.

lower part of the CD while the remaining part of the field is expelled upward (Fig. 1c to d, cf. Fig. 2).

Below the surface, the strong downflow around $x = 0.7$ Mm draws the reconnected magnetic field lines downward (Fig. 1d,e), so that for some time two loops are present. As the downflow decays, the 'magnetic finger' is no longer sustained and the configuration relaxes.

The pressure below the longer loop (between $x = 1$ Mm and $x = 2$ Mm) increases and a vigorous upflow develops, which carries the loop upward until it leaves the CD. As a result of this 'flux reemergence', the initial situation with two strong vertical FSs of opposite polarity is restored.

3.2. The reconnection process

Figure 2 shows the reconnection processes (Fig. 1c and d) with higher temporal resolution. Four snapshots separated by 25 s are plotted. One reconnection site is located between the sheets around $x = 0.7$ Mm and $z > 0.1$ km. The upper parts of the FSs brought together by the flows remain vertical. They rapidly reconnect and form a 'U'-shaped structure which leaves the computational domain through the upper boundary while the surface flows continue to bring together magnetic field lines having opposite polarity.

A second location where reconnection takes place (near $x = 0.8$ km and $z = -0.3$ km, Fig. 2) involves a disconnecting magnetic bubble. Although reconnection is present it does not manage to untie the bubble completely. In contrast to the previously described reconnection the external flow does not bring opposite polarities close enough together. Moreover, the ambient magnetic field around the bubble inhibits the detachment of the bubble.

3.3. Observer's view

Figure 1 shows that the reconnection takes place within the observable layers. It is therefore interesting to relate the dynamics of magnetic elements described above to the view of an idealized observer who is hypothetically able to resolve the sun at the given model resolution of 25 km (= pixel size). Since the observer looses the crucial depth information, 3D space is reduced to a 2D field of view whereas in our 2D simulation it becomes 1D. Figure 3 shows the 1D field of view along the x-axis (horizontal position) and includes the temporal evolution along the y-axis. The grey-scale image corresponds to the vertical magnetic field strength taken at $\log(\tau) = -0.5$, black and white reflect the two polarities.

Figure 3 allows us to follow the evolution of FSs which now appear as magnetic elements (MEs). They repeatedly appear (e.g. $x = 1.4$ Mm, $t = 20$ min) and disappear (e.g. $x = 1.4$ Mm, $t = 35$ min), and opposite polarities are often found to lie close together (e.g. $x = 1.0$ Mm, $t \sim 127$ min). Whether appearance or disappearance of MEs indicates the actual formation or destruction of a FS cannot be derived from the 'magnetogram' since the crucial depth information is lacking and renders the interpretation ambiguous.

Figure 3 also includes information about the vertical velocity structure: the thin contour lines connect spatio-temporal points where the vertical velocity vanishes. While MEs are located in downflows not all downflows harbor a strongly concentrated magnetic field. Note that the formation a new downflow (e.g. $x = 3.5$ Mm, $t = 25$ min) – which occurs when a granule fragments (see, e.g., Ploner et al. (1999)) – is often related to the appearance of a weak bipolar region (Gadun et al. 2001).

We focus now on the recycling process described in the previous sections. For reference, the snapshot of Fig. 1a is taken at $t = 85$ min, and Fig. 1h at $t = 99$ min, the spatio-temporal point where the two FSs come close together (after Fig. 1c) lies near $x = 0.9$ Mm, $t = 90$ min.

Before the opposite polarities merge, the white ME to the right of the merging point seems to fade out and become 'disconnected'. Comparison with Fig. 1a to c reveals the cause of this behavior: the strong surface flow pushes the right FS towards the merging point. Since the ME moves by more than its diameter per stored (not calculated!) time step the white line appears to be misleadingly disconnected.

Shortly before the merging point, the observer first sees two MEs of opposite polarity which vanish abruptly somewhat later suggesting the annihilation of magnetic flux. A few minutes later one polarity reappears, still some minutes later the other polarity reappears, but almost 1000 km to the right of the point at which they merged. The gap in magnetic flux corresponds to the situation in Fig. 1d, where the upper part of the FS has been cut off by reconnection and the magnetic arch has formed below the surface. Later the arch rises ($x = 1.2$ Mm

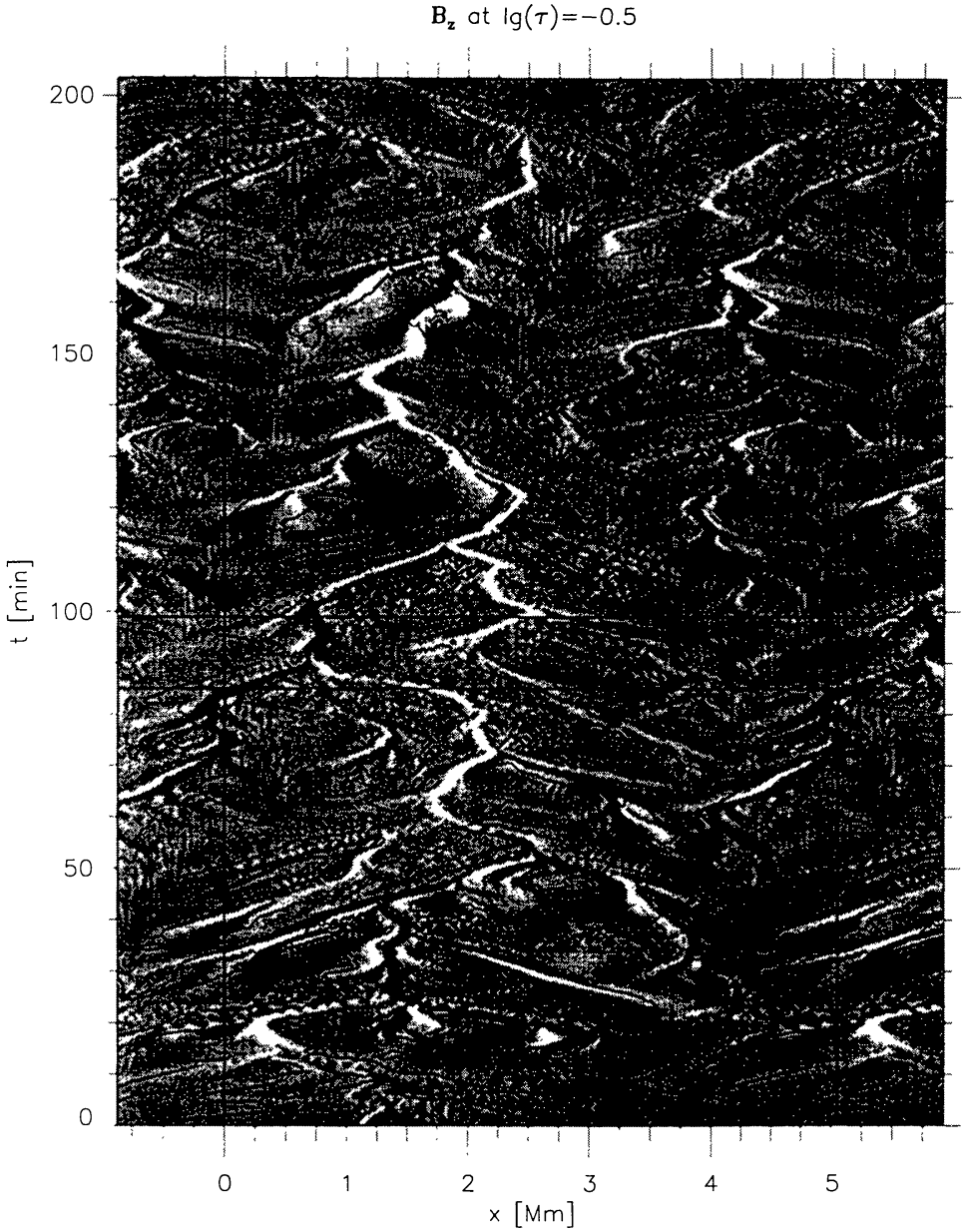

Figure 3. Synthetic magnetogram with null lines of the vertical velocity. Horizontal position is plotted along the x-axis, time increases from bottom to top along the y-axis. The image has been periodically extended outside the thin vertical lines. The grey-scale image displays the vertical magnetic field component, B_z, taken at $\log(\tau) = -0.5$, i.e. somewhat above the visible surface (τ is continuum optical depth at $\lambda = 5000$Å). White and black indicate the different polarities (maximum field strength is ± 2000 G) whereas grey corresponds to zero field strength. The vertical velocity vanishes at the contour lines. The displayed level is given by the upper thick horizontal line drawn in the frames of Fig. 1. Those frames are located between the two horizontal lines of this figure.

in Fig. 1e) and nearly vertical magnetic field lines cross the $\log(\tau) = -0.5$ layers at one of its foot points. Due to the asymmetry in the shape of the arch (the left part rises quicker than the right part) it takes longer until the right foot point becomes visible in a 'magnetogram', which only samples the vertical component of the field at $\log(\tau) = -0.5$. The large distance between the merging point to the freshly emerged white ME reflects the length of the loop.

4. Summary and conclusion

The results presented in this contribution are obtained from a 2D MHD simulation which includes the layers near the solar surface. The novelties of our numerical experiment are that the magnetic field consists of mixed polarity and that the run discussed here covers the extended time span of 3 h solar time.

We describe an example of flux recycling in which two, initially vertical flux sheets (FSs) are pushed together by strong surface flows. Through reconnection a magnetic arch develops below the surface whereas the magnetic field lying in the atmosphere leaves the computational domain through the upper boundary. Inhibited convective upflow enhances the pressure under the magnetic loop and eventually raises it into the atmosphere, so that finally two strong FSs are present, similar to the initial configuration. Magnetic flux has been recycled since no new flux has been produced or has entered through the boundaries. The evolution of the two FSs seen as magnetic elements in a synthetic magnetogram – roughly reflecting the view of an idealized observer – shows that flux seems to disappear (either through cancellation or dissolution) and to reappear later. Comparison with the underlying situation shows that the observer is faced with the changing visibility of the flux. Only if the field lines cross the visible layers nearly vertically the corresponding flux does appear as a magnetic element in the magnetogram. If the field lines are inclined or lie below the visible surface no flux seems to be present in a magnetogram.

Flux recycling events are an efficient mechanism which easily give rise to fictitious disappearance of 'old' and appearance of 'new' flux in magnetograms. Schrijver et al. (1998), e.g., report observational evidence for a high flux emergence rate in the quite Sun and relate this rate to coronal heating. Since they find no evidence for the newly emerged magnetic flux to be retracted below the surface again they postulate that it must reconnect with other flux. The energy released through this reconnection heats the corona. The high flux emergence rate indicates that such a mechanism is at work. Although such an emergence rate may be caused by a 'local' surface dynamo (e.g. Cattaneo 1999) our study shows that flux recycling offers an alternative explanation.

References

Brandt P.N., Gadun A.S. 1995, Kinematika i Fizika Nebes. Tel. 11, no. 4, 44

Cattaneo F. 1999, ApJ, 515, L39

Gadun A.S. 1995, Kinematika i Fizika Nebes. Tel. 11, no. 3, 54

Gadun A.S., Solanki S.K., Johannesson A. 1999, A&A, 350, 1018

Gadun A.S., Solanki S.K., Sheminova V.A., Ploner S.R.O. 2001, Sol. Phys., submitted

Nordlund Å., Stein R.F. 1989, in R. Rutten, G. Severino (eds.), *Solar and Stellar Granulation*, 453, Kluwer Dordrecht

Ploner S.R.O., Gadun A.S., Schüssler M., Solanki S.K. 2001, A&A, in preparation

Ploner S.R.O., Solanki S.K., Gadun A.S. 1999, A&A, 352, 679

Schrijver C.J., Title A.M., Harvey K.L., Sheeley Jr N.R., Wang Y.M., van den Oord G.H.J., Shine R.A., Tarbell T.D., Hurlburt N.E. 1998, Nature, 394, 152

Steffen M., Freytag B. 1991, Rev. Mod. Astron., 4, 43

Steiner O., Grossmann-Doerth U., Knölker M., Schüssler M. 1998, ApJ, 495, 468